IEEE Access
Multidisciplinary | Rapid Review | Open Access Journal

IEEE ON IEEE POWER & ENERGY SOCIETY SECTION

Received December 9, 2020, accepted December 30, 2020, date of publication January 4, 2021, date of current version January 11, 2021.

Digital Object Identifier 10.1109/ACCESS.2020.3048980

Optimization of an Offshore Oilfield Multi-Platform Interconnected Power System Structure

QINGGUANG YU, ZHICHENG JIANG, YUMING LIU, LE LI, AND GAOXIANG LONG
State Key Laboratory of Power System, Department of Electrical Engineering, Tsinghua University, Beijing 100084, China

Corresponding author: Qingguang Yu (yuqingguang@163.com)

This work was supported by the National Key Research and Development Project under Project 2018YFB0904800.

ABSTRACT In recent years, with regional integrated seabed resource exploitation continuing to expand, offshore oilfield power systems have gradually become networked, forming an offshore oilfield multi-platform interconnected power system. In this paper, a two-level optimization model for offshore oilfield multi-platform interconnected power system structure is developed. The lower-level model uses a minimum cut-load cost model that considers load priority to calculate the power outage losses of all N−1 fault conditions. The reliability assessment method helps to achieve a balance between economy and reliability. Additionally, an optimization model simplification method based on graph theory is proposed, and it uses the minimum cost maximum flow (MCMF) algorithm to optimize the power flow of the grid and narrows the problem's solution space. At the end of modeling, a parallel global taboo search algorithm is used to reduce the computational time and improve the probability of finding an optimal solution. Investigations of a real offshore oilfield multi-platform power system verify the accuracy of the model, the simplification method and the parallel global taboo search algorithm.

INDEX TERMS Graph theory, optimization, power system planning, power system reliability.

I. INTRODUCTION

In recent years, with growing demand for resources, the exploitation of seabed resources has become an important part of the world's resource structure. As the primary facilities for the exploitation of seabed oil and gas resources, offshore oilfield platforms have been widely used. The offshore oilfield platform power system, which serves as the energy supply system of offshore oilfield platforms, supplies energy to exploitation and storage equipment and living facilities. Existing offshore oilfield platform power systems contain a single power station platform that supplies power to other platforms through submarine cables. The total load of the power supply system in this mode is typically small: a single generator's output accounted for a high proportion of the total system load, and submarine cable failure would cause power outages in connected platform production and living equipment. All these features lead to poor power supply reliability, poor impact resistance, large equipment start difficulty, etc., which seriously affect the production of offshore oilfield platforms [1], [2]. As the scale of offshore oilfield exploitation continues to expand, the density of offshore oilfield platform distribution continues to increase, gradually forming a regionally integrated model of offshore oilfield exploitation [3]. In this scene, an offshore oilfield platform power system gradually becomes a power grid and transforms from a single generation-radiation power supply to a distributed multi-generation power supply, thus forming an offshore oilfield multi-platform interconnected power system. In an offshore oilfield multi-platform interconnected power system, system capacity is increased, and mutual support is provided among multiple power station platforms, which improves generator utilization efficiency, increases system stability and reliability, and enhances the economic benefits of offshore oilfield. To achieve this goal, it is necessary to optimize the structure of the offshore oilfield multi-platform interconnected power system, which includes both a grid frame and generation expansion planning, to achieve an optimal balance of economy and reliability.

Currently, because offshore oilfield power systems are still being developed into multi-platform interconnected power systems, the scale of offshore oilfield multi-platform

The associate editor coordinating the review of this manuscript and approving it for publication was Emilio Barocio.

interconnection power systems is typically small, and few grid structure options are present, leading to low demand for structural optimization. Therefore, there are few studies that investigate offshore oilfield multi-platform interconnection power system structure optimization. Reference [4] established a power-grid cooperative optimization model for offshore oilfield multi-platform interconnected power systems that considers generator construction costs, submarine cable construction costs, system operating costs and outage loss costs using a hybrid contraption search genetic algorithm. However, this study neglects the influence of submarine cable specifications on the construction cost, and the calculation of outage loss cost is based on the difference between the total installed capacity and the total load to calculate the cut-off load but does not consider outage losses caused by grid capacity limitations in the event of failure; thus, the optimization results have strong limitations.

In the field of power system planning, researchers primarily focus on land-based power systems to perform research. The planning model of related research based on an optimization objective can be divided into economic models [5], [6], reliability models [7], [8], and comprehensive models [9]–[14]. The economic model is the most widely used model, which only considers the investment cost of the generator, the grid frame and the operating cost of the system, and requires the reliability of the system to meet the normal operation condition or pass the N−1 calibration. The reliability model only optimizes the reliability of the system; thus, the optimized scheme also must be checked with an economic metric. Reference [7] selects network destructive measurement indicators to obtain alternative network structures with higher reliability; however, the results obtained from the reliability optimization model typically have high economic costs. The comprehensive model comprehensively considers the economic and reliability optimization models, and considers different indicators in two ways. First, researchers weighted multiple indicators to obtain the objective function. [9], [10] The problem with using this method of managing multiple objectives is how to reasonably determine the weight of different indicators. Also, normalization is required if the order of magnitude of the indicators are different. Second, a multi-objective optimization model is established [11]–[14]; however, this model typically requires Pareto optimality as a stopping criterion, and there are many such Pareto-optimal solutions in the solution space of multi-objective optimization. Thus, it is difficult to obtain a true balance between the multiple objectives in a multi-objective optimization model. In this paper, a comprehensive model is used to balance the two important optimization goals of economy and reliability, where the reliability is represented by the cost of the outage losses, which makes it simple to add up the economy and reliability indicators and avoid the trouble of determining weights.

The power system planning optimization model is a MINLP problem, which can be solved directly only by heuristic algorithms. Heuristic algorithms include genetic algorithm [15], [16], particle swarm algorithm [17], simulated annealing algorithm [18], ant colony algorithm, taboo search [4], etc. These algorithms have few requirements for optimization models and are insensitive to the optimization model size. However, these algorithms cannot guarantee finding the global optimum solution, that is, the algorithm is easy to fall into a local optimum. Improvements in heuristic algorithms have been made by adjusting the parameters within an acceptable time frame to try to avoid the algorithm falling into a local optimum, yielding good results from an engineering perspective. To obtain an accurate optimal solution, many studies have simplified mixed-integer nonlinear models using methods like segmental linearization [10], using DC power flow equations [18] or retaining quadratic terms instead of AC power flow equations [19], to step down the order of higher-order constraints in the optimization model. These simplified models are typically mixed integer quadratically constrained programs (MIQCP) [5], [19] with quadratic terms in the constraints or mixed integer linear programming (MILP) [20]–[22], allowing commercial solvers such as CPLEX and Gurobi to be used to obtain exact solutions. However, these optimization models that can be simplified often tend to only consider the economics of the solution (i.e., they use economic models that only require the solution to work properly in normal condition in terms of reliability). Therefore, in this paper, to fully consider the reliability of the power system, the structure optimization model of an offshore oilfield multi-platform interconnected power system remains a mixed-integer nonlinear model; however, the model uses the DC power flow equation instead of the AC power flow equation for simplification. Also, a parallel global taboo search algorithm is used to reduce the computation time of the optimization problem.

The remainder of this paper is organized as follows. Section II describes the offshore oilfield multi-platform power system structure optimization model. Section III introduces the simplification of the optimization model using graph theory. A parallel global taboo search algorithm is proposed in Section IV, and Section V demonstrates the effectiveness of the optimization model and the algorithm by the results achieved from a real application on an offshore oilfield multi-platform interconnected power system in China. Conclusions are then drawn in Section VI.

II. OPTIMIZATION MODEL

The offshore oilfield multi-platform interconnected power system structure optimization model is a two-level optimization model. The upper level model sets the total annual cost of the scheme as the optimization objective, and the lower level optimization model optimizes the annual outage loss cost of the scheme. However, the upper level optimization model provides the grid scheme and unit allocation scheme to the lower optimization model, and the optimization results of the lower level optimization model are components of the objective function of the upper optimization model.

A. UPPER LEVEL OPTIMIZATION MODEL

1) OBJECTIVE FUNCTION OF UPPER LEVEL

The upper level optimization model views economy as the optimization objective, and the economic items considered consist of investment cost, system operation and maintenance cost and outage loss cost. The investment cost includes generator investment cost and submarine cable investment cost. The system operation and maintenance cost includes generator maintenance cost, generator fuel cost and submarine cable maintenance cost. Considering that the offshore oilfield power system primarily uses self-produced crude oil and natural gas to generate electricity, the power generation cost is low. Additionally, the offshore oilfield interconnected power system, which is interconnected by many single-source radial traditional offshore oilfield platform power systems, is small in scale. In normal conditions, the power transmission distance is short, the network loss is small, and the difference of generator fuel cost between different grid schemes is small and negligible. Additionally, the cost of submarine cable maintenance is small compared to the generator maintenance cost, which is also negligible. Therefore, the system operation and maintenance costs primarily consists of the generator overhaul maintenance costs. Outage loss costs include the loss of oil and gas production caused by system failure. Because system failure is effectively random, outage loss costs are calculated for the expected outage loss costs in a year.

The objective function of the upper level optimization model is shown in (1):

$$\min \mathrm{TC} = \frac{i(1+i)^N}{(1+i)^N - 1}(\mathrm{GIC} + \mathrm{LIC} + \mathrm{GMCP}) + \mathrm{OC} \quad (1)$$

where TC indicates the total cost per year; GIC, LIC and GMCP represent generator investment cost, submarine cable investment cost and all generator overhaul maintenance costs over the planning period discounted to the present value, respectively; OC indicates the expected outage losses per year due to power failure. $i(1+i)^N/((1+i)^N-1)$ is discount factor from present value to equivalent year value; i is the discount rate; and N is the planning year.

The generator investment cost (GIC) can be calculated as shown in (2), where X_i^{gen} represents the number of new generators installed on platform i, c^{gen} represents the price of one generator and Ω_b represents the platform set:

$$\mathrm{GIC} = \sum_{i \in \Omega_b} X_i^{\mathrm{gen}} c^{\mathrm{gen}} \quad (2)$$

The present value of the generator overhaul and maintenance cost (GMCP) is calculated by the formula shown in (3), where GMC is the cost of a single generator overhaul and k is the kth generator overhaul:

$$\mathrm{GMCP} = \sum_{5k \le N} \frac{\mathrm{GMC}}{(1+i)^{5k}} \quad (3)$$

The total investment cost of the submarine cable includes the investment cost of the new cable and the enhanced cable (LIC), as shown in (4):

$$\mathrm{LIC} = \sum_{ij \in \Omega_l} \alpha_{ij} c_{ij}^{(k)} l_{ij} \quad (4)$$

where Ω_l represents the set of the optional corridor existing lines; ij represents a corridor or existing line; i, j represents the platform at both ends of the corridor or existing line; and l_{ij} is the length of the corridor or existing line ij; For the optional corridor ij, when making the decision to erect the line in the overhead corridor ij, α_{ij} equals 1; otherwise α_{ij} equals 0. k is a variable for corridor ij that represents the type of new line to be constructed. For the existing line ij, when deciding to enhance the existing line, α_{ij} equals 1; otherwise, α_{ij} equals 0. In this case, k is a constant that is based on the type of the existing line. $c_{ij}^{(k)}$ represent the investment cost per unit length of the kth type of submarine cable.

Using historical failure statistics of the offshore oilfield multi-platform interconnected power system, the loss caused by the generator and submarine cable N−1 failure is shown to make up a large proportion of the total loss. Therefore, the outage loss cost primarily includes the loss of capacity due to generator and submarine cable N−1 failure in a year, thus fully describing the reliability of the power system and avoiding a detailed analysis of the type of failure that may significantly increase computation time. The formula shown in (5) describes this loss, where Ω_{N-1} represents the set of N−1 fault of power system, λ_i represent the occurrence number of failure i per year, MTTR_i indicates the repair time of failure i and VOLL_i shows the production loss per unit time due to power outages caused by failure i:

$$\mathrm{OC} = \sum_{i \in \Omega_{N-1}} \lambda_i \mathrm{MTTR}_i \mathrm{VOLL}_i \quad (5)$$

2) CONSTRAINTS OF THE UPPER LEVEL MODEL

In the upper-level optimization model, the optimization solution is subject to many constraints, including those faced by the structure optimization problem of the land power system and those imposed by many ocean-specific conditions. A qualified solution must satisfy the following constraints.

(1) System normal operation constraint. The offshore oilfield multi-platform interconnected power system structure optimization model coordinates the economy and reliability of the scheme by considering the cost of power outage in the objective function. However, a qualified scheme must satisfy the most basic requirement of system normal operation (i.e., three constraints).

The first includes power balance constraints. As shown in (6), each platform must balance power during normal operation. The DC power flow equation is used in this study to simplify calculations, where B is the system conduction matrix during normal operation, θ is the node voltage phase vector during normal operation, and P^{gen} is the platform generator output vector during normal operation and P^{load} is the platform load vector:

$$B\theta - P^{\mathrm{gen}} = P^{\mathrm{load}} \quad (6)$$

The second includes generator output constraints. As shown in (7), the generator output of the power station platform must be below the installed capacity of the platform. In the formula, $P^{\text{gen\_rate}}$ is the rated power of a single generator:

$$0 \le P_i^{\text{gen}} \le X_i^{\text{gen}} P^{\text{gen\_rate}} \tag{7}$$

The third includes cable capacity constraints. As shown in (8), the power delivered by the line is limited, and exceeding the power limit will cause the cable to heat up and burn out. In this formula, θ_i and θ_j are node voltage phases at nodes i and j, respectively. $x_{ij}^{(k)}$ represents the reactance per unit length when the kth submarine cable is selected in the corridor ij, and $P^{(k)}$ represents the rated transmission capacity of the kth submarine cable:

$$\left| \frac{\theta_i - \theta_j}{l_{ij} x_{ij}^{(k)}} \right| \le P^{(k)} \tag{8}$$

(2) Constraints on the number of generators on the platform: As shown in (8), the cost of the offshore oilfield platform is high, and the cost of the platform increases markedly as the platform space and load increase due to limited platform space, and the fact that the number of platform generators is not allowed to exceed the maximum allowable value of the platform. $N_i^{\text{gen,max}}$ indicates the maximum number of generators on platform i:

$$0 \le X_i^{\text{gen}} \le N_i^{\text{gen,max}} \tag{9}$$

(3) Grid topology constraints: The offshore oilfield multi-platform interconnected power system is interconnected by multiple single-source radiating offshore oilfield platform power systems, and the grid structure is typically radiating or single-ring. Thus, the optimized solution must meet the grid structure requirements.

B. LOWER LEVEL OPTIMIZATION MODEL

1) OBJECTIVE FUNCTION OF LOWER LEVEL

The lower optimization model is a minimum cut-load model that considers load priority and is used to calculate the loss of outage capacity for a specific N−1 fault condition.

The load on the offshore oilfield multi-platform interconnected power system can be divided into public and production loads. The public load is the load in the subsequent processing process for oil extraction and has a higher priority than the production load because if the processing process is interrupted by a power outage, oil extraction must also be stopped. The production load is closely related to oil extraction and is proportional to the amount of crude oil extracted. However, due to the different depths of each platform from the seabed reservoir and the variations in oil content of crude oil, the same production load on different platforms to obtain oil and gas production typically leads to different oil and gas output. After analyzing the oil and gas capacity and load data of each platform, the production load of each platform can be prioritized based on the ratio of oil and gas output to production load of each platform. Therefore, in case of system failure, the load can be cut based on the load priority of each platform; thus, the loss caused by power outage can be reduced by arranging the load cut of the platform with a low ratio of oil and gas output to production load, while the public load is supported. Based on the production load cut during system failure, the VOLL of the failure can be calculated as shown in (10):

$$\text{VOLL} = \sum_{i \in \Omega_b} \frac{c_i^{\text{output}} P_{i,\text{production}}^{\text{shedding}}}{P_{i,\text{production}}} \tag{10}$$

where c_i^{output} represents the value of oil and gas output of platform i, $P_{i,\text{production}}$ indicates the production load on platform i, and $P_{i,\text{production}}^{\text{shedding}}$ refers to the amount of shedding production load on platform i.

The objective function of the minimum load-cutting model that considers load priority levels based on these load-cutting rules is shown in (11):

$$\min C = \text{VOLL} + F \sum_{i \in \Omega_b} P_{i,\text{public}}^{\text{shedding}} \tag{11}$$

where C is a load-shedding evaluation index, where the smaller the index, the lower the priority of the load cut by the current load-shedding scheme; F is a constant used to distinguish the priority of production load from public load, which must be greater than the ratio of oil and gas capacity to production load for all platforms; and $P_{i,\text{public}}^{\text{shedding}}$ is the amount of shedding public load on platform i.

2) CONSTRAINTS OF THE LOWER LEVEL MODEL

Similar to the upper level optimization model, the solution of the minimum cut-load model that considers load priority must satisfy the constraints shown in (12-15), where (12) is the power balance constraint, (13) is the load cut constraint, (14) is the generator output constraint, and (15) is the cable capacity constraint. All variables have similar meaning to those used in the upper level optimization model but consider the N−1 fault condition:

$$\begin{aligned} &B_{\text{fault}} \theta_{\text{fault}} - P_{\text{fault}}^{\text{gen}} - P_{\text{production}}^{\text{shedding}} - P_{\text{public}}^{\text{shedding}} \\ &\quad = P_{\text{production}} + P_{\text{public}} \end{aligned} \tag{12}$$

$$0 \le P_{\text{production}}^{\text{shedding}} + P_{\text{public}}^{\text{shedding}} \le P_{\text{production}} + P_{\text{public}} \tag{13}$$

$$0 \le P_{i,\text{fault}}^{\text{gen}} \le X_{i,\text{fault}}^{\text{gen}} P^{\text{gen\_rate}} \tag{14}$$

$$\left| \frac{\theta_{i,\text{fault}} - \theta_{j,\text{fault}}}{l_{ij} x_{ij}^{(k)}} \right| \le P^{(k)} \tag{15}$$

III. MODEL SIMPLIFICATION METHOD BASED ON MCMF

A. IDEA OF MODEL SIMPLIFICATION METHOD

In the offshore oilfield multi-platform interconnection power system structure optimization model, the decision variable of the corridor is represented by a Boolean variable, and the type of the new line to the line is represented by an

integer variable with a value range of $1\sim k$. The line to be enhanced is also represented by a Boolean variable. For the optimization problem with l corridors, m lines that can be enhanced, and k optional types of submarine cables, there is a coupling relationship between the two decision variables of the corridors and the optional types of submarine cables when considering the corridor and the line for enhancement. Also, the solution space of the grid part is $2^m(k+1)^l$ and increases exponentially with the number of corridors and existing lines. Thus, if the model is not processed, and the problem is solved directly by heuristic algorithm, it will yield inefficient computation and typically lead the algorithm to fall into the local optimum solution.

For offshore oilfield multi-platform interconnected power systems, the line to be enhanced is determined by the grid structure. Based on the chosen corridor, the basic structure of the grid is determined, and bottlenecks in the existing lines can be found through the optimization of the power flow of the grid. After the chosen corridor and the line to be enhanced are determined, the type of submarine cable to be used in the corridor can be calculated based on the optimization of the grid power flow. Because the structure optimization model focuses on the reliability of the system in the N−1 fault state, all N−1 fault states must be considered in optimizing the grid power flow. After simplifying the decision variables using these methods, the solution space size of the decision variables in the grid part of the structure optimization model is reduced to 2^l.

B. APPLICATION OF MCMF

In the method shown above, both the identification of the line to be enhanced and the determination of the line type require the optimization of the grid power flow. Power flow optimization when the grid is not fully defined must ensure that power outage losses and grid construction costs are minimized. The traditional minimum cut-load model cannot optimize the power flow while meeting the requirements of both objectives; however, the network flow model can meet these requirements through the design of the weight of the edge. For a radial grid structure, using the minimum cost max flow (MCMF) to solve the offshore oilfield multi-platform interconnected power system network flow model and the flow of the edge is the real line flow of the corresponding power system open loop operation. The network flow modeling of power stations, load platforms and line based on the characteristics of the power flow optimization model of the offshore oilfield multi-platform interconnected power system is introduced below.

As shown in Figure 1, the power station platform is modeled as a directed edge from the source node to the power station node in the network flow model, and the capacity of the edge is the capacity of the generators installed on the platform. The weight of the edge is 0, and the edge that is full of flow indicates that the power node cannot take more load when the output of generator reaches capacity.

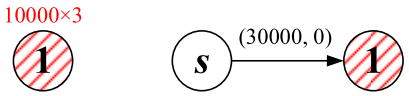

FIGURE 1. Network modeling of power stations.

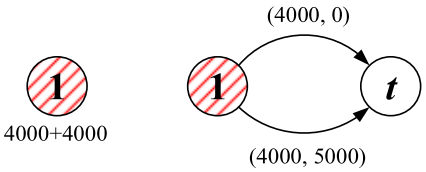

FIGURE 2. Network modeling of load platforms.

As shown in Figure 2, the load platform in the network flow model is modeled as a directed edge from the load node to the sink node. The capacity of the edge is the size of load. The edge that is full of flow indicates that the load operates at full power. The weight of the edge is related to the load type. The load on an offshore oilfield platform can be divided into public and production loads, and each offshore oilfield platform may include one or both loads. The public load provides power for the processing of oil extracted from multiple offshore oilfield platforms; thus, the public load power outage will cause all offshore oilfield platforms to be unable to produce normally. The production load is primarily responsible for the exploitation of oil, and when there is a shortage of power supply, the production load of certain low-priority platforms can be cut based on the ratio of output value to production load on each platform. Therefore, in case of insufficient power supply, the public load has a higher priority than the production load, and the production load of each platform is prioritized by its ratio from output value to production load. In Figure 2, the load of platform 1 includes a 4000-kW public load and a 4000-kW production load, and the ratio of the output value to the production load is 0.5. The priority of the production load is primarily represented by the weight of the edges in the network flow model, and the edge with low weight corresponds to the load with high priority. Thus, for the public load, its corresponding edge has a weight of 0 when modeling. With the production load, its corresponding edge has a weight of the ratio of the output value to the production load; however, to avoid the production load priority being perturbed by line side weights, the unit capacity consumption load must be multiplied by a large number, which is chosen to be 10,000, as shown in Figure 2.

As shown in Figure 3, the line in the network flow model is modeled as two edges in opposite directions. The edge with the same direction as the line flow is the positive edge, and the opposite edge is the negative edge. Either of the two edges can be considered to be the positive edge in the initial state. In the residual network, the capacity and weights of the two edges are related to the type of line and the flow f on the line.

In the offshore oilfield multi-platform interconnected power system, the existing lines are divided into lines that can

FIGURE 3. Network modeling of line.

or cannot be enhanced. Lines that can be enhanced indicate that when there is a capacity bottleneck in the line, a new line of the same size is allowed to be built in the corridor to run in parallel with the original line. In the residual network, the residuals and weights of the two edges corresponding to the lines can be enhanced are shown in Table 1. The residuals and weights of the two edges corresponding to the lines that cannot be enhanced are shown in Table 2, and the residuals and weights of the two edges corresponding to the lines to be constructed are shown in Table 3.

TABLE 1. Relationship between edge parameters and flow of lines can be enhanced in residual network.

Line flow	Positive side residuals	Positive side weights	Negative side residuals	Negative side weights
f=0	c	l	c	l
0<f<c	c-f	l	f	-l
f=c	2c-f	100l	f	-l
c<f<2c	2c-f	100l	f-c	-100l
f=2c	0	∞	f-c	-100l

TABLE 2. Relationship between edge parameters and flow of lines cannot be enhanced in residual network.

Line flow	Positive side residuals	Positive side weights	Negative side residuals	Negative side weights
f=0	c	l	c	l
0<f<c	c-f	l	f	-l
f=c	0	∞	f	-l

TABLE 3. Relationship between edge parameters and flow of lines to be constructed in residual network.

Line flow	Positive side residuals	Positive side weights	Negative side residuals	Negative side weights
f=0	c_{max}	10l	c_{max}	10l
0<f<c_{max}	c_{max}-f	10l	f	-10l
f=c	0	∞	f	-10l

With these modeling approaches, the output of the power station platform will be below the installed capacity of the platform, the maximum cut load will be below the load size, and the line current will be below the maximum capacity of the line. Because the system is a radial grid, the number of independent nodes and independent edges of the system are equal, and the voltage phase angles of all other nodes can be derived from the flow of each edge after determining the reference node. Therefore, the optimization results obtained from the MCMF algorithm satisfy the DC power flow equation and meet the constraints of normal operation or N−1 fault conditions. In the MCMF model of the power flow of the offshore multi-platform interconnected power system, the lines in the system are divided into three priorities. The existing lines are set as the first priority, thus fully utilizing the capacity of the existing lines and improving the line utilization. Because the cost of lines to be constructed increases as the line diameter increases, the lines to be constructed are set as the second priority, thus limiting the power flow of the new lines as much as possible and reducing the diameter of the new lines. Because the lines to be enhanced require the construction of submarine cables of the same length and size as the original lines, which are typically more expensive for the same length, the lines to be enhanced are set as a third priority, thus reducing the construction of lines to be enhanced. Different priorities can be distinguished by multiplying the weight of the corresponding edge by the priority factor; however, for lines within the same priority, the priority is distinguished by line length, which requires the load to be supplied by the nearest power station platform, thereby optimizing the power flow of the system.

IV. PARALLEL GLOBAL TABOO SEARCH ALGORITHM

To shorten the solution time of the optimization model and improve the global search capability of the taboo search algorithm, this paper integrates the ideas of the taboo search algorithm, particle swarm algorithm and simulated annealing algorithm to propose a parallel taboo search algorithm.

A. TRADITIONAL TABOO SEARCH ALGORITHM

The steps of applying traditional taboo search algorithm to solve the offshore oilfield multi-platform interconnected power system structure optimization model are shown in Figure 4.

(1) Coding of optimization variables: After the simplification described in Section III, the only independent decision variable of the offshore oilfield multi-platform interconnected power system structure optimization model is the selection of the corridor; thus, it is possible to use a binary coding method, where 0 indicates that the corridor is not selected, and 1 indicates that it is selected.

(2) Taboo search initialization: The initial solution can be generated using a random spanning tree algorithm to generate a radial grid, and then a corresponding number of lines can be added randomly based on the number of contact lines to form the initial grid. The Kruskal algorithm [23] can be used for random tree generation by treating each node as a tree without edges in the initial state. Then, the algorithm picks an edge randomly from the edge set. If the nodes at both ends of this edge are located in the same tree, then the edge is removed from the edge set; otherwise, the tree where the two endpoints are located is merged, and the edge is removed from the edge set concurrently. The selected edges are also added to the tree. Edges are selected randomly from the set of all edges, and these operations are repeated until a tree

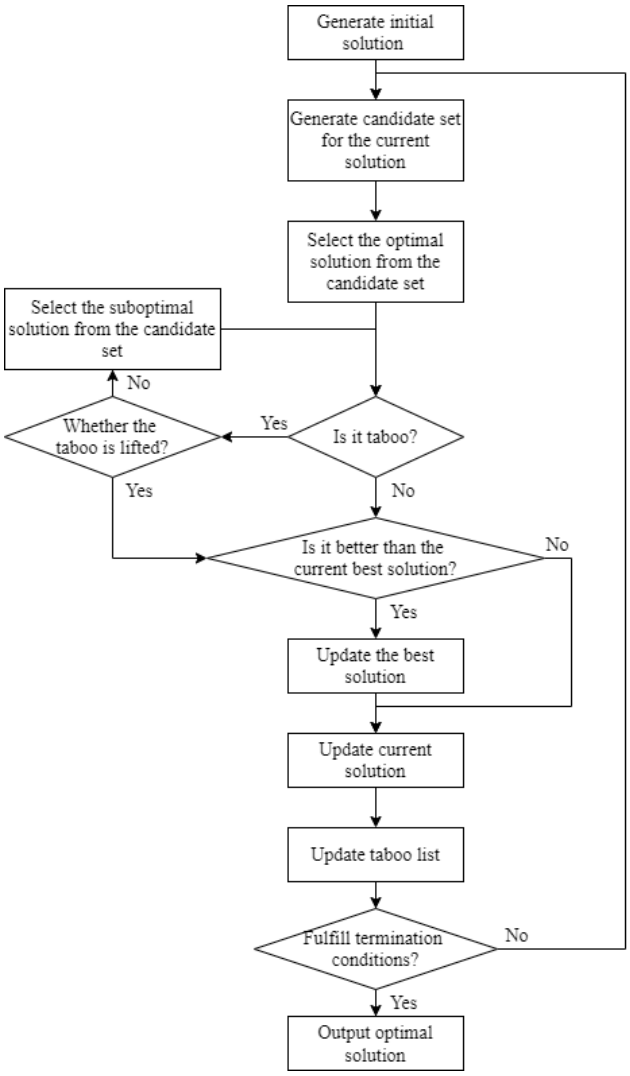

FIGURE 4. Process of traditional taboo search algorithm.

containing all nodes is created, at which point the tree is randomly generated. An initial solution can be obtained by randomly selecting connecting branches based on the number of contact lines to be added to the set of branches. This initial solution is evaluated, and the initial solution is set as the optimal solution. The taboo list length is then set, and the initial taboo list is emptied.

(3) Generate candidate set: The algorithm uses a neighborhood search based on the current solution to generate candidate solutions, which indicates repeatedly acting neighborhood action on the current solution to generate a series of candidate solutions. In the offshore oilfield multi-platform interconnected power system structure optimization model, only grid structure schemes are randomly searched, and the neighborhood of a grid structure scheme can be defined as all grid structure schemes with only two different lines. Neighboring action makes the grid structure from the current scheme to its neighbors in another scheme. The operation process is actually a branch exchange process that uses graph theory to add a random edge in the current scheme and find all loop edges. A loop edge excluding the new edge is then randomly removed from the grid structure scheme to ensure grid structure connectivity.

(4) Evaluate all solutions of the candidate set.

(5) Update the current solution: Select the neighbor in the candidate set that has the best score and is not in the taboo list or meets the amnesty criterion as the current solution.

(6) Update the best solution by comparing the updated current solution with the best solution.

(7) Update the taboo list: Add the neighborhood action from the current solution before the update to the current solution updated and unban the neighborhood action at the end of the taboo list.

(8) Check the termination condition: The termination condition of taboo search algorithm is typically set as reaching maximum number of iterations or maximum number of consecutive iterative steps of which the best solution remains constant. If the termination condition is met, the taboo search is stopped immediately and the optimal solution is output; otherwise, return to step (3) to start a new round of search.

B. PARALLEL GLOBAL TABOO SEARCH ALGORITHM

Drawing from the particle swarm algorithm, the core strategy of the parallel global taboo search algorithm is to execute multiple groups of taboo searches in parallel, and after each completed neighborhood search, the evaluated optimal scheme found by each group of taboo searches is sorted to select the best scheme to be passed to each group of taboo searches. When the next neighborhood search generates a candidate set, except for the group whose best solution equals the global best solution, other groups of taboo searches are not allowed to swap out the lines that they share with the global optimal scheme when using the branch exchange method to act on neighborhood actions. This method can accelerate the convergence and efficiency of the algorithm by guiding the candidate set generation with the global best solution for each group of taboo search, thus reducing computation time.

However, the strict use of globally optimal scheme to guide neighborhood actions can lead the algorithm into local optimal solutions. What's more, the strict restriction of neighborhood actions may lead to the generation of a large number of identical neighborhood solutions, resulting in inefficient searching. So there needs to be a principle to allow neighborhood actions not guided by global optimal scheme. This paper draws on the idea of simulated annealing algorithm to solve this problem. At the beginning of the iteration, the neighborhood search is designed to have a greater probability of not receiving guidance from the global best solution to expand the random search capability of the algorithm. The formula for this probability is shown in (16):

$$p = \max\left[e^{-\frac{kg}{G}}, 0.2\right] \tag{16}$$

where g is the number of iterations performed, G is the maximum number of iterations designed for taboo search,

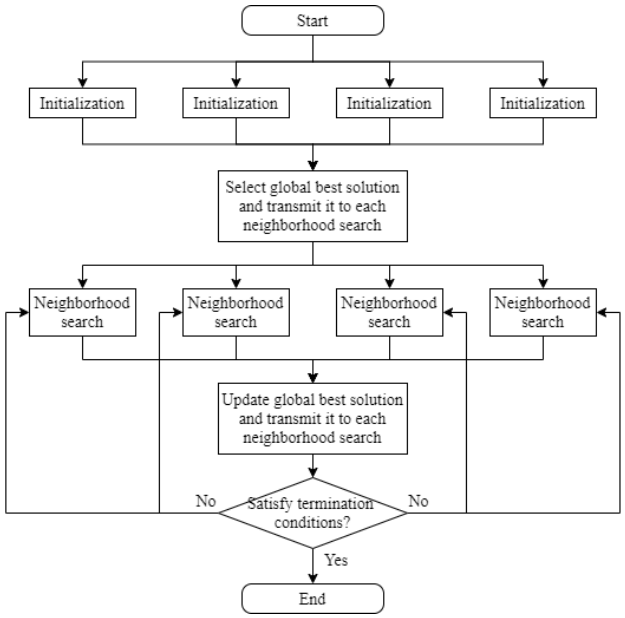

FIGURE 5. Process of parallel global taboo search algorithm.

and k is the parameter which can adjust the speed of probability being smaller. Thus, in the initial run of taboo search, $e^{-kg/G}$ is near 1, and the taboo search is not guided by the global best solution, which ensures that the algorithm has a good global search capability. As the number of iterations increases, $e^{-kg/G}$ decreases. To avoid strict restrictions on neighborhood action leading to generate a large number of the same neighborhood solution, the minimum probability of taboo search rejecting the guidance of the global optimal solution is 0.2.

The process of parallel global taboo search is shown in Figure 5, where there are four groups of parallel taboo searches. The initialization corresponds to steps (1)∼(2) introduced in subsection A, and the neighborhood search corresponds to steps (3)∼(7). It can be noticed that the parallel global taboo search also adds an additional step relative to the traditional taboo search. The global optimal solution is transmitted once after each completed neighborhood search for all groups. In addition, the termination criterion for global taboo search is marginally different from taboo search, where the termination criterion for global taboo search is to reach the set maximum number of iterations or the optimal solution of all groups being the same.

V. CASE STUDY

A. INTRODUCTION OF THE CASE STUDY

Figure 6 shows a case adapted from a real offshore oilfield multi-platform power system in the South China Sea, where nine platforms have been built. Platform 1 is a terminal processing plant built on an island and equipped with seven generators with a rated capacity of 6000kW. Platforms 2 and 6 are existing power station platforms with three generators with a rated capacity of 4261kW and two generators with a rated

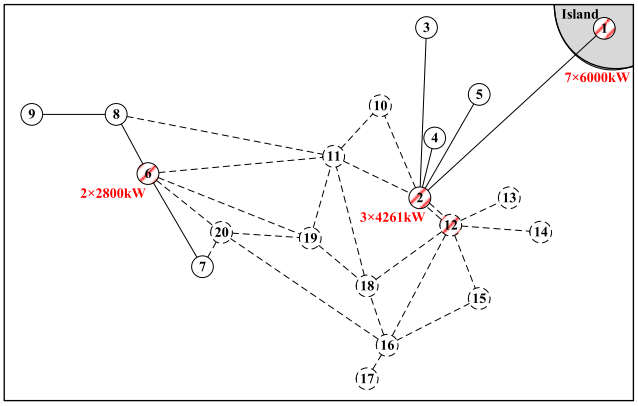

FIGURE 6. Offshore oilfield multi-platform interconnected power system to be optimized.

capacity of 2800kW, respectively. Platforms 3∼5 and 7∼9 are wellhead platforms, and Platforms 1∼5 and 6∼9 have been connected to form two independent radial power systems. In this case study, oil exploitation is expanding, and it is expected that, in the future, a total of 11 platforms will be built, of which Platform 12 is a new power station platform. And according to the overall load of the system, generators with a rated capacity of 7600kW are expected to be installed on Platform 12. The connection relations and types of the submarine cable built in the system, information of the optional corridor, platform load information, submarine cable parameters, and generator parameters are shown in the Appendix.

The cable failure rate and repair time used in the structure optimization model are fit according to historical cable failure statistics for the sea area where the planning system is located, and the relationship between cable failure rate and cable length is shown in (17):

$$\lambda(L) = \begin{cases} 0.0175 & L < 9.33\text{km} \\ 0.0037L - 0.017 & L \geq 9.33\text{km} \end{cases} \tag{17}$$

The relationship between the cable repair time and length is shown in (18):

$$\text{MTTR}(L) = 117.75 + 26.201L \tag{18}$$

Other parameters used in the structure optimization model are shown in Table 4.

B. IMPACT OF RELIABILITY ASSESSMENT METHODS ON OPTIMIZATION RESULTS

This subsection focuses on the impact of using two different reliability assessment methods in structure optimization model on the final optimization results. The first is to calculate the outage losses for each N−1 fault condition using the minimum cut-load model proposed in this paper that considers load priority levels. The second is to calculate the outage losses for each N−1 fault condition using the method of the literature [4] and then discount the outage losses using the power outage rate. The final optimization results

TABLE 4. Other parameters used in the structure optimization model.

Parameter	Value
Oil price	2868.4 yuan/m^3
Gas price	1.54 yuan/m^3
Number of generator failures per year	1.59
Average generator repair time	27.31h
Discount rate	7%
Planning year	15

using the two reliability assessment methods are shown in Figures 7 and 8, respectively, and the corresponding costs for the two results are shown in Table 5.

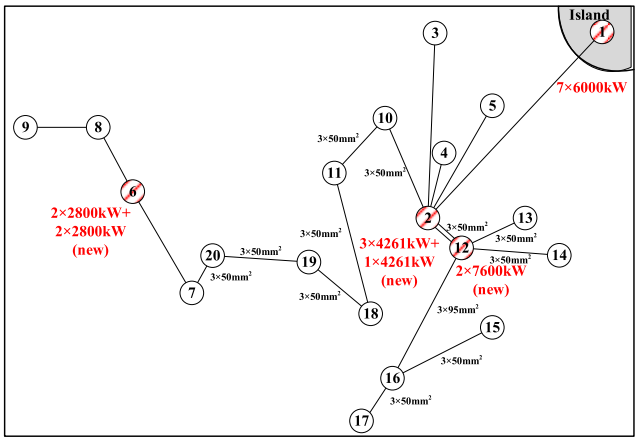

FIGURE 7. Optimization results using reliability assessment method 1.

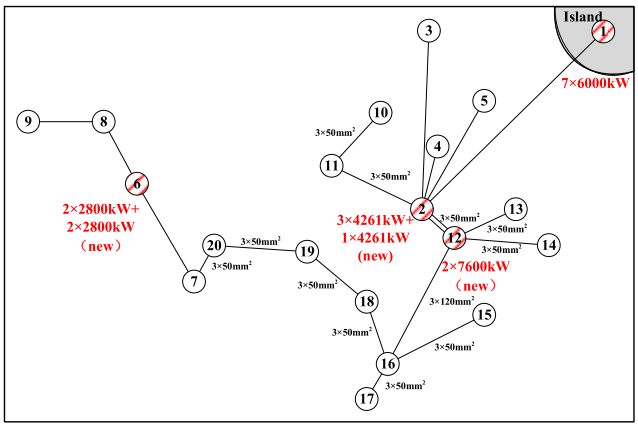

FIGURE 8. Optimization results using reliability assessment method 2.

It can be found that the submarine cable investment cost of the scheme obtained using the first reliability assessment method in the structural optimization model is 6.8067 million yuan, which is marginally higher than that of the scheme obtained using the second method, which is 6.5146 million yuan. However, from the perspective of reliability, the outage

TABLE 5. Cost of optimization results using different reliability assessment methods.

	GIC+GMCP (million yuan)	LIC (million yuan)	OC (million yuan)	TC (million yuan)
1	23.142	6.807	4.061	34.010
2	23.142	6.515	6.440	36.097

loss cost of the scheme obtained using the first reliability assessment method is 4.0611 million yuan, which is apparently lower than that of the scheme obtained using the second method, which is 6.44 million yuan. In summary, compared to the reliability evaluation method used in reference [4], the reliability evaluation method proposed in this paper can find a solution that balances economy and reliability better in the structure optimization model.

C. EFFECT OF MODEL SIMPLIFICATION METHOD ON SOLVING EFFICIENCY

This subsection investigates the effect of the simplification method on solving efficiency. The model is solved using the taboo search algorithm, where MATLAB is the software environment, an Intel Core i7-8750H is the hardware platform processor, and 16GB of memory are used. The number of neighbors searched per neighborhood search in taboo search is set to 15, and the taboo search termination criterion is the optimal solution not changed for 10 iterations. The two groups of taboo searches are repeated 50 iterations, respectively, and the results are shown in Table 6.

TABLE 6. Comparison of optimization information with or without simplification.

	Decision variables not simplified	Decision variable simplified
Probability of finding the optimal frame	2% (1/50)	72% (36/50)
Average total cost (million yuan)	35.572	34.097
Total cost standard deviation(million yuan)	1.189	0.196
Average number of iterations	39.48	10.42
Standard deviation of number of iterations	15.84	5.17
Average calculation time(s)	32.32	12.47
Standard deviation of calculation time(s)	13.18	6.03
Average search time per iteration(s)	0.82	1.20

Table 5 leads to the following conclusions:

(1) After simplifying the decision variables of the optimization model, the time for a single evaluation solution increases. The average time to evaluate 15 neighbors in an iteration with the simplification is 1.20 seconds, an increase of 46.22% compared to the average evaluation time

of 0.82 seconds without simplification. However, the number of iterations required for the algorithm to converge with the simplification decreases from an average of 39.48 iterations to an average of 10.42, a decrease of 73.61%. Thus, the average taboo search time with simplification is 12.47 seconds, which is 61.42% lower than the average evaluation time of 32.32 seconds without simplification, which is a significant improvement in the overall efficiency of the calculation.

(2) The solution space is reduced, and the stability of the search results is indirectly improved by simplifying the decision variables. Only 1 of 50 taboo searches find the optimal solution without simplification, and the average total cost of 50 searches is 35.57 million yuan with a standard deviation of 1.19 million yuan. After simplifying the decision variables, the average total cost of the 50 searches was 34.09 million yuan, a relative reduction of 4.33%, and the standard deviation was 1.96 million yuan, a relative reduction of 83.49%.

D. EFFECT OF PARALLEL GLOBAL TABOO SEARCH ON SOLVING EFFICIENCY

This subsection examines the performance of the parallel global taboo search algorithm in terms of computational efficiency and global search capability. To compare the solution performance of parallel global taboo search and traditional taboo search algorithms, two sets of tests are designed. The first set of tests uses the traditional taboo search algorithm with 15 neighbors. The second set of tests uses the parallel global taboo search algorithm, which performs three sets of taboo searches in parallel, with five neighbors per set of taboo searches. The tests are repeated 50 times, and the results are shown in Table 7.

TABLE 7. Comparison of optimization information using traditional taboo search and parallel global taboo search.

	Decision variables not simplified	Decision variable simplified
Probability of finding the optimal frame	72% (36/50)	94% (47/50)
Average total cost (million yuan)	34.097	34.028
Total cost standard deviation(million yuan)	0.196	0.083
Average number of iterations	10.42	12.48
Standard deviation of number of iterations	5.17	5.11

Analysis of the data shows that after using the global taboo search, the algorithm's global search capability is markedly improved, with 47 of 50 taboo searches being able to search for the optimal solution, an increase of 27.03% compared to 36 without the global taboo search. However, in terms of computational efficiency, there is also a marginal increase in the time taken for the global taboo search. The sets using parallel global taboo search algorithm takes an average of 12.48 iterations to find the best solution, a 19.77% increase relative to the 10.42 iterations with the traditional taboo search.

VI. CONCLUSION

Considering that existing structure optimization studies of offshore oilfield multi-platform interconnected power systems do not describe the balance between economy and reliability, a two-level single-objective offshore oilfield multi-platform power system structure optimization model is developed and tested in this study. The minimum cut-load cost model considering the load priority level is used in the model to calculate the outage losses of the system under all N−1 fault states, which helps to achieve a better balance between economy and reliability.

A model simplification method based on graph theory is also shown to simplify the decision variables. The simplification method uses MCMF to optimize the power flow of the grid, which significantly reduces computation time and improves the probability of finding the global optimal solution.

Additionally, a parallel global taboo search algorithm is applied to solve the optimization model to accelerate the calculation of the optimization model. Also, the case based on the real offshore oilfield multi-platform power system verifies the effect of the optimization model, the model simplification method and the parallel global taboo search algorithm.

TABLE 8. Existing submarine cable data.

Start platform	End platform	Length(km)	Diameter (mm^2)
1	2	32.5	185
2	3	12	50
2	4	2.8	50
2	5	7.1	75
6	7	5.6	50
6	8	2.6	50
8	9	10	50

TABLE 9. Alternative corridors data.

Start platform	End platform	Length (km)	Start platform	End platform	Length (km)
2	8	19.5	11	19	6.1
2	10	6.9	12	13	4.92
2	11	6.5	12	14	9.6
2	12	0.05	12	15	9.8
6	11	12	12	16	7.4
6	19	6.8	12	18	6.2
6	20	3.8	15	16	6.1
7	20	1.8	16	17	1.76
8	11	15	16	18	3.7
8	19	8.5	16	20	13.1
10	11	5.8	18	19	3.7
11	18	6.9	19	20	5.3

TABLE 10. Load and output of each platform.

Platform	Production load(kW)	Public load(kW)	Oil daily output(m^3)	Gas daily output(10^4 m^3)
1	0	17344	0	0.00
2	1500	6872	492	20.20
3	100	0	174	0.17
4	2352	0	927	35.86
5	387	0	135	0.24
6	3406	0	767	6.99
7	450	0	318	1.00
8	2333	0	416	1.92
9	1000	0	0	3.00
10	387	0	916	4.38
11	506	0	290	0.82
12	0	5253	0	0.00
13	2720	0	905	18.75
14	1204	0	531	2.76
15	790	0	497	0.85
16	5186	0	479	9.63
17	4003	0	581	12.79
18	1032	0	432	6.76
19	350	0	242	0.68
20	4148	0	590	1.83

TABLE 11. Parameters of submarine cable.

Number	Diameter (mm^2)	Maximum current(A)	Cable cost (10^4 ¥ /km)	Construction cost(10^4 ¥ /km)
1	50	197	71.00	28.80
2	75	239	81.60	30.70
3	95	281	92.00	32.60
4	120	315	102.70	34.50
5	150	350	113.40	36.20
6	185	388	127.00	38.10
7	240	440	149.00	40.20
8	300	484	173.00	42.00
9	400	537	190.00	43.00

TABLE 12. Parameters of generator.

Numb er	Rated capacity (kV)	Investment cost(10^4 ¥)	Overhaul cost(10^4 ¥)	Overhaul year
1	12700	6322.50	1264.50	5
2	10500	5690.25	1138.05	5
3	7600	4560.00	912.00	5
4	6000	3840.00	768.00	5
5	4281	2911.08	582.22	5
6	2800	1988.00	397.60	5

For future research directions, with the introduction of offshore wind power, shore power and energy storage devices in offshore oilfield multi-platform interconnected power system, further investigation of the optimization of this kind of power system structure can be also conducted. This is projected to be of great practical significance in guiding the planning of new forms of offshore oilfield multi-platform interconnected power systems.

APPENDIX

See Tables 8–12.

REFERENCES

[1] X. Li, "Overview of offshore electric systems," *Power Syst. Clean Energy*, vol. 32, no. 2, pp. 1–7, Feb. 2016.
[2] Q. Li, X. Li, and C. Wei, "Offshore oil and gas field cluster power networking technology," *Shipbuilding China*, vol. 22, no. 1, pp. 218–223, Jul. 2011.
[3] C. Zhao, "Regional integration development mode of Bohai oilfields and its application," *China Offshore Oil Gas*, vol. 28, no. 3, pp. 218–223, Jun. 2016.
[4] D. Sun, X. Xie, J. Wang, Q. Li, and C. Wei, "Integrated generation-transmission expansion planning for offshore oilfield power systems based on genetic tabu hybrid algorithm," *J. Mod. Power Syst. Clean Energy*, vol. 5, no. 1, pp. 117–125, Jan. 2017.
[5] J. F. Franco, M. J. Rider, and R. Romero, "A mixed-integer quadratically-constrained programming model for the distribution system expansion planning," *Int. J. Electr. Power Energy Syst.*, vol. 62, pp. 265–272, Nov. 2014.
[6] G. Munoz-Delgado, J. Contreras, and J. M. Arroyo, "Distribution system expansion planning considering non-utility-owned DG and an independent distribution system operator," *IEEE Trans. Power Syst.*, vol. 34, no. 4, pp. 2588–2597, Jul. 2019.
[7] K. Li, J. Wang, and L. Yang, "Distribution network structure optimization based on multi-scene destructivity analysis," *Autom. Electr. Power Syst.*, vol. 38, no. 1, pp. 34–37,81, Jan. 2014.
[8] W. M. Lin, C. D. Yang, and M. T. Tsay, "Distribution system planning with evolutionary programming and a reliability cost model," *IEE Proc.-Gener., Transmiss. Distrib.*, vol. 147, no. 6, pp. 336–341, Nov. 2000.
[9] R. C. Lotero and J. Contreras, "Distribution system planning with reliability," *IEEE Trans. Power Del.*, vol. 26, no. 4, pp. 2552–2562, Oct. 2011.
[10] X. Jin, Y. Song, W. Yang, Y. Lv, and Z. Li, "Research on planning strategy to achieve high reliability for urban distribution systems," in *Proc. IEEE 3rd Int. Electr. Energy Conf. (CIEEC)*, Beijing, China, Sep. 2019, pp. 1143–1147.
[11] S. Kazmi, M. Shahzad, and D. Shin, "Multi-objective planning techniques in distribution networks: A composite review," *Energies*, vol. 10, no. 2, p. 208, Feb. 2017.
[12] S. Ganguly, N. C. Sahoo, and D. Das, "Multi-objective planning of electrical distribution systems using dynamic programming," *Int. J. Electr. Power Energy Syst.*, vol. 46, pp. 65–78, Mar. 2013.
[13] A. M. Cossi, L. G. W. Da Silva, and R. A. R. Lazaro, "Primary power distribution systems planning taking into account reliability, operation and expansion costs," *IET Gener., Transmiss. Distrib.*, vol. 6, no. 3, pp. 274–284, Jan. 2012.
[14] K. Silivanh, S. Premrudeepreechacharn, and K. Ngamsanroaj, "Distribution system planning and development for supporting economic—Social growth in Luangprabang province Lao PDR," in *Proc. IEEE 6th Int. Conf. Power Syst. (ICPS)*, New Delhi, India, May 2016, pp. 1–4.
[15] S. Heidari and M. Fotuhi-Firuzabad, "Integrated planning for distribution automation and network capacity expansion," *IEEE Trans. Smart Grid*, vol. 10, no. 4, pp. 4279–4288, Jul. 2019.
[16] H. M. A. Ahmed, A. B. Eltantawy, and M. M. A. Salama, "A planning approach for the network configuration of AC-DC hybrid distribution systems," *IEEE Trans. Smart Grid*, vol. 9, no. 3, pp. 2203–2213, May 2018.
[17] R. Li, W. Wang, and M. Xia, "Cooperative planning of active distribution system with renewable energy sources and energy storage systems," *IEEE Access*, vol. 6, pp. 5916–5926, 2018.
[18] S. Kirkpatrick, C. D. Gelatt, and M. P. Vecchi, "Optimization by simulated annealing," *Science*, vol. 220, no. 4598, pp. 671–680, May 1983.
[19] R. A. Jabr, "Polyhedral formulations and loop elimination constraints for distribution network expansion planning," *IEEE Trans. Power Syst.*, vol. 28, no. 2, pp. 1888–1897, May 2013.

[20] S. Haffner, L. F. A. Pereira, L. A. Pereira, and L. S. Barreto, "Multistage model for distribution expansion planning with distributed generation—Part I: Problem formulation," *IEEE Trans. Power Del.*, vol. 23, no. 2, pp. 915–923, Apr. 2008.
[21] M. A. Alotaibi and M. M. A. Salama, "An incentive-based multistage expansion planning model for smart distribution systems," *IEEE Trans. Power Syst.*, vol. 33, no. 5, pp. 5469–5485, Sep. 2018.
[22] M. Jooshaki, A. Abbaspour, M. Fotuhi-Firuzabad, M. Moeini-Aghtaie, and M. Lehtonen, "MILP model of electricity distribution system expansion planning considering incentive reliability regulations," *IEEE Trans. Power Syst.*, vol. 34, no. 6, pp. 4300–4316, Nov. 2019.
[23] B. Joseph Kruskal, "On the shortest spanning subtree of a graph and the traveling salesman problem," *Proc. Amer. Math. Soc.*, vol. 7, no. 1, pp. 48–50, Feb. 1956.

QINGGUANG YU received the Ph.D. degree in electrical engineering from Tsinghua University, Beijing, China, in 1994. He is currently an Assistant Professor with Tsinghua University. His research interests include smart microgrid control strategy and NILM application in power grid.

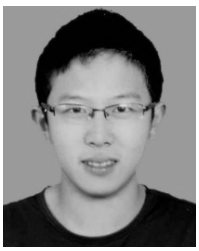

ZHICHENG JIANG received the bachelor's degree from the Department of Electrical Engineering, Tsinghua University, China, in 2019, where he is currently pursuing the master's degree. His research interests include distribution network expansion planning and hybrid renewable energy microgrid control strategy.

YUMING LIU received the bachelor's degree in electrical engineering from the Harbin Institute of Technology, China, in 2018. He is currently pursuing the master's degree with Tsinghua University. His research interests include distribution network economic evaluation and hybrid renewable energy microgrid control strategy.

LE LI received the bachelor's degree from North China Electric Power University, Beijing, China, in 2020. He is currently pursuing the master's degree with Tsinghua University. His research interests include hybrid renewable energy microgrid control strategy and NILM application in power grid.

GAOXIANG LONG received the master's degree from the Department of Electrical Engineering, Tsinghua University, China, in 2020. His research interests include distribution network expansion planning and smart microgrid planning.